Basis set study of classical rotor lattice dynamics

James B. Witkoskie, Jianlan Wu, and Jianshu Cao[a)]
Department of Chemistry, Massachusetts Institute of Technology, Cambridge, Massachusetts 02139

(Received 2 July 2003; accepted 30 December 2003)

The reorientational relaxation of molecular systems is important in many phenomenon and applications. In this paper, we explore the reorientational relaxation of a model Brownian rotor lattice system with short range interactions in both the high and low temperature regimes. In this study, we use a basis set expansion to capture collective motions of the system. The single particle basis set is used in the high temperature regime, while the spin wave basis is used in the low temperature regime. The equations of motion derived in this approach are analogous to the generalized Langevin equation, but the equations render flexibility by allowing nonequilibrium initial conditions. This calculation shows that the choice of projection operators in the generalized Langevin equation (GLE) approach corresponds to defining a specific inner-product space, and this inner-product space should be chosen to reveal the important physics of the problem. The basis set approach corresponds to an inner-product and projection operator that maintain the orthogonality of the spherical harmonics and provide a convenient platform for analyzing GLE expansions. The results compare favorably with numerical simulations, and the formalism is easily extended to more complex systems. © *2004 American Institute of Physics.* [DOI: 10.1063/1.1649735]

I. INTRODUCTION

Reorientational relaxation of molecular systems is important in understanding many processes, including dielectric relaxation, solvation dynamics, electron transfer, and critical behavior in liquid crystals.[1–5] Reorientational relaxation has been used as a probe of polymer melts near the glass transition because the rotational motion explores the heterogeneity of local dynamics on long time scales. Studies of rotational motion at the single molecule level demonstrate heterogeneous nonexponential relaxation and possible domain switching in these glassy systems.[6,7] Since fragile glass forming liquids have fairly isotropic interactions, the behavior of the reorientational relaxation in these systems compared with strong liquids may be significantly different, and the differences may be responsible for some of the properties of the glass phase.[8] Dipolar reorientational relaxation of solvents is also important in understanding the structure and function of proteins, proton transfer, solvation of ions, and many other phenomenon that are important to biological processes.[9–16] The reorientational relaxation is also important in interpreting spectroscopy of these complex systems with optical measurements that probe the orientations of transition dipoles.[17]

These applications motivate us to study the reorientational relaxation of a model lattice system, where the molecules are free rotors fixed on a perfectly ordered lattice.[1,2,10–12,14–16,18–22] Time scale separation justifies neglecting translational motion because the reorientational motion is often much faster. Even more simplistic models with limited orientations successfully explained observations of electron transfer reactions and solvation dynamics.[4,23] The molecules interact with each other through a bilinear tensor interaction, $\mu_i \mathbf{T}_{ij} \mu_j$, where i and j denote positions on the lattice and μ_i is the orientation of the molecule at that position. Usually, the interaction tensor $\mathbf{T}_{ij}$ is only a function of the distance between two molecules, and their orientation with respect to the relative position vector. The model allows simple incorporation of an external potential that linearly couples to the orientation of the rotors with a position dependence, but this paper omits this addition for simplicity. Under these interactions, the system undergoes rotational Brownian motion,

$$\partial_t G(\{\Omega_i\},t) = D_0 \sum_i [\nabla^2_{\Omega_i} G(\{\Omega_i\},t) + \nabla_{\Omega_i}[G(\{\Omega_i\}) \nabla_{\Omega_i} \beta V(\{\Omega_i\})]]. \quad (1)$$

The orientation of molecule $i=\{i_x,i_y,i_z\}$ is specified by a set of angles Ω_i. The Green's function is G with a free diffusion constant, D_0, and inverse temperature, β. The potential βV is $\Sigma_{i,j} \mu_i \mathbf{T}_{i,j} \mu_j$, and ∇_{Ω_i} is the rotational diffusion operator.

Simulations using similar lattice solvents characterize the solvation dynamics and thermodynamics of complex systems.[13,24,25] These simulations are more realistic than a dielectric continuum, but not as computationally expensive as molecular dynamics simulations with explicit solvent. To make a comparison between real systems and simulations with lattice solvents, one must explore the properties of the lattice solvent and compare them with more realistic simulations and experiments. Simulations by Papazyan and Maroncelli and by Zhou and Bagchi demonstrated that the model of a Brownian dipolar lattice shows many of the properties of more realistic dipolar liquid systems, such as water, includ-

a)Electronic mail: jianshu@mit.edu

ing non-Debye relaxation that fits the Davidson–Cole dielectric response function, which is often used in the analysis of data from real dipolar systems.[10–12]

The Brownian dipolar lattice has an extensive history. The thermodynamics of this system was studied by Rosenberg and Lax with a high temperature expansion.[19–21] Erzan and Stell used a variational theory to approximate the low temperature behavior of a similar dipolar lattice system, and Høye and Stell used the linear hypervertex approximation to find the ferroelectic phase transition for off-lattice dipolar hard sphere systems, which have been extensively studied by many authors, including Nienhuis and Deutch.[26–28] Using a similar approach, Zwanzig studied the dielectric relaxation of this system.[1,2] Titulaer and Deutch also investigated this system with high temperature expansions to develop a relationship between dielectric relaxation and time correlation functions.[22,29] More recently, Loring and Mukamel used the dipolar lattice to describe the solvation of ions, which Papazyan and Maroncelli studied with a Brownian dynamics simulation.[12,14] Berne, and later Bagchi, Chandra, and Rice applied a time-dependent density functional theory to study a similar system.[15,16,30] Their work elucidated the role of interactions as well as translational and rotational diffusion on deviations from Debye relaxation. Several other simulations on this system reveal the role of phase transitions in the dielectric response and quantify non-Debye relaxation.[31,32]

As discussed in Appendix C, the high temperature, T, expansion for the dipolar lattice starts from the simple isotropic solution of the high temperature phase and systematically incorporates corrections of order T^{-n1}. These solutions are asymptotic to the high temperature solution and may not extrapolate well into finite temperatures. To correct this difficulty, several authors used projection operator techniques to derive a memory kernel that contains the contributions from interactions between rotors.[10,11,33] We refer to this approach as the standard generalized Langevin equation (GLE) approach because the equations have the same form as those derived from the Liouville equation, except there is no random force and the frequency term is replaced by a decay term. Evaluation of the memory kernel resulting from the GLE approach requires a leading order perturbation expansion, which can also possess some difficulties with extrapolation to finite temperatures. As a result, the agreement between the simulation and the perturbation expansion for the dipoles on a lattice breaks down for moderate dipolar interactions, especially in the long time regime.[10,11] The asymptotic nature of these perturbation expansions implies that additional terms in the perturbation series will not necessarily improve the agreement.

The difficulty with traditional perturbation solutions motivates us to explore a basis set approach to Brownian dynamics of interacting rigid rotors on a lattice. In a companion paper, we use a similar approach to study the facilitated kinetic Ising model.[34] In analogy to the use of a basis set in quantum mechanics, we introduce a complete basis set and attempt to diagonalize the diffusion operator within a subspace of the basis set. The basis set gives stability to the equations by partially renormalizing the perturbation expansion, which makes convergence to the finite temperature solution more probable. This renormalization comes from capturing the contributions from collective motions within the truncated basis set. The other perturbation methods incorporate these additional interactions by considering two particle correlations, then three particle correlations, and the sequence continues and results in a failure to capture collective motions at finite order.

The truncated basis set expansion method evaluates the eigenfrequency and memory kernel of the generalized Langevin equation (GLE) by directly incorporating the collective motions of the particles in the system. Unlike the traditional projection operator techniques, the equilibrium distribution contributes to the initial conditions only and are not part of the definition of the memory functions. As will be discussed in Sec. VI, the difference comes from defining a different projection operator, which does not depend on equilibrium so that this approach can be used in systems that are far from equilibrium. The standard GLE approaches with a perturbation expansion to a finite order more closely resemble self-consistent mean field theories, where the particles move in a time dependent potential created by the equilibrium many-body mean field effects. The mean field can give good agreement for short times, but it may fail for longer time scales, where collective motions become important.

This paper shows that the projection operator techniques are much more versatile than one expects from examining the standard GLE approaches. Standard GLE uses a specific basis set and inner product. As discussed in Appendix A, the equations for GLE may not directly write out the higher order basis functions, but one can easily use basis set completeness to show that standard GLE approaches assume a specific basis set and inner-product. The dynamics do not depend on the specific form of the basis set or inner-product, which determine the projection operators. As with all inner-product spaces, the inner-product and the basis set define the space. If two spaces describe the same physical system, the operators in one space must translate into operators in the other space. However, one can never evaluate the equations exactly and the chosen basis set and inner-product influences the accuracy of the approximations.

The choice of the inner-product space (basis set and inner-product) can help reveal certain physics. The standard GLE approach chooses the inner-product as the integral between two elements with a weighting by the equilibrium distribution. For the lattice rotor problems discussed below, one generally cares about orientational correlations functions. The natural basis set for measuring these quantities is the product of spherical harmonics for each rotor in the lattice (see Sec. II). The inner-product with the weighting by the equilibrium distribution destroys the orthogonality of this basis set. In principle one can use Gram–Schmidt procedures to restore orthogonality, but the new inner-product space has a complicated inner-product, which results in complicated projection operators in terms of the quantities that we want to evaluate—the correlations between various spherical harmonics.

If the inner-product does not include the equilibrium distribution, the orthogonality of the spherical harmonics is

maintained for all interactions and temperatures. Orthogonal transformations to other observables are not complicated by the equilibrium distribution. An example in Sec. III A shows that we can easily determine both the vector dependent relaxation and the single rotor relaxation by simple transforms. This vector dependent relaxation can give insight into various collective processes including the validity of ''Onsager's inverted snowball effect.''[35] We can also prepare the system in a nonequilibrium initial condition—applying a strong electric field for negative time and then turning the field off at $t=0$ is an example—and watch the system relax. Standard GLE approaches restrict themselves to fluctuations around equilibrium. The equilibrium independent inner-product space may not be the best choice for all applications, but one should consider the possibility of using inner-products other than those used in standard GLE approaches. In the end, the inner-product, and therefore the projection operator, should be determined by the physics that one wants to reveal.

As a proof of principle, we use the equilibrium independent inner-product to study a simpler system than the dipolar lattice since numerical simulations are easier and the equations are simpler to interpret. The equilibrium independent inner-product allows us to easily explore the vector dependence of the relaxation and explore the role of coupling between different basis elements in the relaxation of the system. The coupling to different basis elements correspond to different relaxation mechanisms, and can give better physical insight into the behavior of the system. Applications to more complicated systems will be addressed in future work. We restrict ourselves to a two dimensional lattice with the molecular orientations also in the plane so that each molecule is described by a single angle, θ_i. The interactions are nearest neighbors (NN) with a directional dependence that resembles the dipolar interaction in two dimensions,

$$\beta V = \sum_{i,j=\mathrm{NN}} -J(\mu_i\cdot(i-j))(\mu_j\cdot(i-j))+J\mu_i\cdot\mu_j$$

$$= \sum_i 2J\cdot\cos(\theta_i+\theta_{i+\binom{0}{1}})-2J\cdot\cos(\theta_i+\theta_{i+\binom{1}{0}}). \quad (2)$$

This interaction is chosen because the tensors $\mathbf{T}_{ij}$ have many properties that appear in the dipolar tensor, including $\Sigma_j \mathbf{T}_{ij}=0$. Zwanzig performed a direct perturbation expansion of the dipolar tensor and many of his expressions do not depend on the exact form of $\mathbf{T}_{ij}$ so we can directly compare our basis set approach with Zwanzig's perturbation expansion.[1,2] These properties also simplify evaluation of these expressions, since it makes cancellations among different terms more apparent.

Redefining the angles that correspond to the μ_i's maps this problem into the classical xy plane rotor model with the exotic Kosterlitz–Thouless phase transition $[(\theta_{2i}\rightarrow\theta_{2i}),\ (\theta_{2i+\binom{1}{0}}\rightarrow-\theta_{2i+\binom{1}{0}}),\ (\theta_{2i+\binom{0}{1}}\rightarrow\pi-\theta_{2i+\binom{0}{1}})$, and $(\theta_{2i+\binom{1}{1}}\rightarrow\theta_{2i+\binom{1}{1}}-\pi)]$.[36–38] Although we are mainly concerned with the high temperature basis set expansion, we address some of the issues associated with a spin-wave basis set in the low temperature regime in Sec. V. Similar to the results for the dipolar lattice, the short time behavior displays a many-body effect on the motions of a single dipole, but longer time behavior depends on collective motions.[10,11,15] Unlike the dipolar system, our system cannot be frustrated so the single rotor correlation function is not slower than the many-body correlations. We show that the harmonic modes of spin-waves capture both the short and the longer time scale behavior with deviations in the intermediate time regime. The success of spin waves in the low temperature regime and the single particle basis set in the high temperature regime is similar to local clustering modes versus hydrodynamic modes discussed in applications of mode coupling theory.[33,39]

The rest of the paper is organized as follows: Section II introduces the basis set formalism in a general context for lattice rotor models. In Sec. III we demonstrate application of this formalism to the specific model discussed above. Section IV presents a numerical comparison between the direct perturbation expansion, a memory kernel expansion, and the truncated basis set. For completeness, we discuss the low temperature spin-wave approximation in Sec. V and conclude in Sec. VI.

II. CORRELATION FUNCTIONS AND THE BASIS SET

In this section we will introduce the application of the truncated basis set method to a three-dimensional lattice with arbitrary bilinear interactions. The discussion is general, but we apply these methods to a simpler two-dimensional system in Sec. III because we can perform accurate simulations of this system. The important measured quantities are the correlation functions of the orientations of the rigid rotors. In this paper, we calculate the autocorrelation function of a single rotor. This correlation function is important in understanding the dielectric properties of neat solvents and in interpreting two-dimensional spectroscopy of a solute in a dilute solvent, such as HDO in D_2O. Choosing the direction that we measure the rotor's orientation as the z axis, the autocorrelation function can be written as

$$\overline{\mu_i^z(t)\mu_i^z(0)}=\overline{\cos(\theta_i(t))\cos(\theta_i(0))}$$

$$=\frac{4\pi}{3}\overline{Y_{1,0}(\Omega_i(t))Y_{1,0}(\Omega_i(0))}, \quad (3)$$

where the overbar denotes expectation, $\mu_i^z(t)$ is the z component of the rotor's orientation vector, $\theta_i(t)$ is the corresponding angle in polar coordinates, and $Y_{1,0}$ is the spherical harmonic, $Y_{1,0}=\sqrt{3/(4\pi)}\cos(\theta)$. In fact, all important observable can be expressed in terms of correlations between elements of the orthogonal basis set,

$$\chi(\{l_i,m_i,\Omega_i(t)\})=\prod_i Y_{l_i,m_i}(\Omega_i(t)). \quad (4)$$

For the single-particle autocorrelation function, all rotors are in the $Y_{0,0}=1/\sqrt{4\pi}$ state except for rotor i. The correlation between two basis elements, $\chi(\{l_i,m_i,\Omega_i(t)\})$ and $\chi(\{l_i',m_i',\Omega_i(t')\})$ can be formally written as

$$\int \prod_i \frac{d\Omega_i}{4\pi} \chi^\dagger(\{l_i,m_i,\Omega_i\}) \times \exp[\mathbf{D}(t-t')]\chi(\{l_i',m_i',\Omega_i\})\rho_{\mathrm{eq}}(\{\Omega_i\}), \quad (5)$$

where $\mathbf{D}$ is the diffusion operator defined by the Green's function and $\rho_{\mathrm{eq}}(\{\Omega_i\})$ is the equilibrium distribution. If we have time translational invariance, we can set $t'=0$. The diffusion operator is not Hermitian and must be applied to the right. By defining an inner-product, $\langle A|B\rangle = \int (d\Omega_j/(4\pi))A^\dagger B$, and using bra-ket notation, we rewrite the equation in terms of the adjoint operator, $\mathbf{D}^\dagger$,

$$\langle \chi(\{l_i,m_i,\Omega_i\})|\exp[\mathbf{D}t]\chi(\{l_i',m_i',\Omega_i\})\rho_{\mathrm{eq}}(\{\Omega_i\})\rangle = \langle \exp[\mathbf{D}^\dagger t]\chi(\{l_i,m_i,\Omega_i\})|\chi(\{l_i',m_i',\Omega_i\})\rho_{\mathrm{eq}}(\{\Omega_i\})\rangle \quad (6)$$

with

$$\mathbf{D}^\dagger = D_0 \sum_i [\nabla_{\Omega_i}^2 - [\nabla_{\Omega_i}\beta V(\{\Omega_i\})]\nabla_{\Omega_i}]. \quad (7)$$

The equilibrium and dynamic parts can be separated by using basis set completeness, $\mathbf{I}=\Sigma|\chi(\{l_i,m_i,\Omega_i\})\rangle \times\langle\chi(\{l_i,m_i,\Omega_i\})|$, which results in the expression

$$\langle \exp[\mathbf{D}^\dagger t]\chi(\{l_i,m_i,\Omega_i\})|\chi(\{l_i',m_i',\Omega_i\})\rho_{\mathrm{eq}}(\{\Omega_i\})\rangle = \sum_{l_i'',m_i''} \langle \exp[\mathbf{D}^\dagger t]\chi(\{l_i,m_i,\Omega_i\})|\chi(\{l_i'',m_i'',\Omega_i\})\rangle \times\langle \chi(\{l_i'',m_i'',\Omega_i\})|\rho_{\mathrm{eq}}(\{\Omega_i\})|\chi(\{l_i',m_i',\Omega_i\})\rangle. \quad (8)$$

In this expression, $\rho_{\mathrm{eq}}(\{\Omega_i\})$ can be considered a self-adjoint operator. The equilibrium contribution is the initial conditions for the propagation of the equation and can be replaced by nonequilibrium initial conditions. The high temperature limit, $\beta=0$, corresponds to free diffusion with a diagonal correlation function,

$$\langle \exp[-\mathbf{D}^\dagger t]\chi(\{l_i,m_i,\Omega_i\})|\chi(\{l_i',m_i',\Omega_i\})\rho_{\mathrm{eq}}(\{\Omega_i\})\rangle = \prod_i \delta_{l_i,l_i'}\delta_{m_i,m_i'} \exp[-\lambda(\{l_i,m_i\})t], \quad (9)$$

where $\lambda(\{l_i,m_i\})=D_0\Sigma_i l_i^2$. Since each dipole is acting independently in this high temperature limit, the decay of the dipolar orientation, $\langle\cos(\theta_i(t))\cos(\theta_i(0)\rangle$, will decay as a single exponential which is consistent with normal Debye behavior. Adding interactions will naturally cause deviations from this behavior.

As in quantum mechanics, if the angular dependence of the potential comes from a bilinear form, we can express the potential as the product between $Y_{1,m}(\Omega_i)$ and $Y_{1,m}(\Omega_j)$ spherical harmonics. The potential couples basis set elements whose angular momentum quantum numbers, l_i, differ by one on two rotors or by two on a single rotor. This scenario is similar to the spirit of mode coupling with the hierarchical coupling structure. For a weak potential, the fast decay of the diffusion term $\exp[-\lambda(\{l_i,m_i\})]$ dominates the modes with large $\lambda(\{l_i,m_i\})$ values and the potential term can be neglected. These observations give a natural scheme for performing a basis set expansion for high temperatures. We truncate the summation in Eq. (8) at the point where the diagonal free diffusion term dominates the coupling between basis set elements. Then we approximately diagonalize this truncated basis set with respect to the diffusion operator and solve for the equation of motion.

The simplest interpretation of this approach is a matrix propagation scheme with the matrix elements of $\mathcal{M}$ determined by $\langle\mathbf{D}^\dagger\chi(\{l_i,m_i,\Omega_i\})|\chi(\{l_i',m_i',\Omega_i)\rangle$ and initial conditions determined by $\langle\chi(\{l_i',m_i',\Omega_i\})|\rho_{\mathrm{eq}}(\{\Omega_i\})|\chi(\{l_i'',m_i'',\Omega_i)\rangle$. As demonstrated in the next section, diagonalization of even the simple two dimensional requires some approximations, but excellent agreement with simulation at fairly strong interactions requires only a few basis elements. The truncated basis set approach outlined above applies to many different systems. The only requirements are a complete basis set and local coupling between elements of the basis set. If this is not the case for the chosen basis set, a different basis set should be explored. As an example, in Sec. V we use the collective spin wave basis set to capture the long time low temperature behavior of a single rotor. These results demonstrate the importance of choosing a proper basis set.

The basis set approach can also be interpreted as a projection operator technique with projection operators defined by $\Sigma_i|\chi_i\rangle\langle\chi_i|$, where the sum is over the elements that span the range of the projection. This simple result is discussed in Appendix A. Appendix A also shows the equivalence of the standard GLE approach to this projection operator. This result is expected since most of the results of the projection operator approaches do not depend on the specific form of the projection operator.

III. SINGLE ROTOR CORRELATIONS IN THE TWO-DIMENSIONAL SHORT RANGE MODEL

To maintain consistency between the two-dimensional model and the general framework outlined in the preceding section, we define our single particle basis set for the two-dimensional model with the sine and cosine functions. In three dimensions, the cosine function corresponds to the $Y_{l,0}$ spherical harmonic. The choice of these trigonometric functions makes it easier to visualize. To simplify notation, we define $\vec{\mu}_{li}^{\,1}=\cos(l\cdot\theta_i)$ and $\vec{\mu}_{li}^{\,2}=\sin(l\cdot\theta_i)$, and denote the set $\{\vec{\mu}_{li}^{\,1},\vec{\mu}_{li}^{\,2}\}$ as $\vec{\mu}_{li}$, and $\vec{\mu}_{1i}$ as $\vec{\mu}_i$. With these definitions, the potential is

$$\beta V = J\sum_{i,j} \vec{\mu}_i\cdot\mathbf{T}_{i,j}\cdot\vec{\mu}_j \quad (10)$$

with

$$\mathbf{T}_{i,j}=\begin{pmatrix}1 & 0\\ 0 & -1\end{pmatrix}(\delta_{j,i\pm\binom{1}{0}}-\delta_{j,i\pm\binom{0}{1}}). \quad (11)$$

The Kronecker delta ensures nearest-neighbor interactions with the proper directional dependence. From our definitions of $\vec{\mu}_{li}$, we build an orthogonal basis set, which can be blocked into several groups,

$$
\begin{aligned}
&A_0=1,\\
&(A_1)_i^{\alpha}=\sqrt{2}\vec{u}_i^{\alpha},\\
&(A_2^1)_{ij}^{\alpha\beta}=2\vec{\mu}_i^{\alpha}\vec{\mu}_j^{\beta}\quad (j>i),\quad (A_2^2)_i^{\alpha}=\sqrt{2}\vec{\mu}_{2i}^{\alpha},\\
&(A_3^1)_{ijk}^{\alpha\beta\gamma}=2^{3/2}\vec{\mu}_i^{\alpha}\vec{\mu}_j^{\beta}\vec{\mu}_k^{\gamma}\quad (k>j>i),\\
&(A_3^2)_{ij}^{\alpha\beta}=2\vec{\mu}_{2i}^{\alpha}\vec{\mu}_j^{\beta}\quad (j\neq i),\quad (A_3^3)_i^{\alpha}=\sqrt{2}\vec{\mu}_{3i}^{\alpha},\\
&\ldots .
\end{aligned}
\tag{12}
$$

This basis set is orthonormal with respect to the inner-product $\langle A|B\rangle=\int\Pi_i(d\theta_i/(2\pi))A^{\dagger}B$, which is not the thermal equilibrium average used in most GLE formalisms. Throughout this paper italic characters, such as *i*, *j*, and *k* refer to a lattice position, *x* and *y*, and the greek characters, such as α, β, γ refer to the two vector components, sin or cos, so that $\vec{\mu}_{li=(0)}^{\alpha=1}=\cos(l\cdot\theta_{(0)}^{0})$ and $\vec{\mu}_{li=(0)}^{\alpha=2}=\sin(l\cdot\theta_{(0)}^{0})$, where $l=1$, 2, 3 in the basis set defined above and we drop the 1 for the $l=1$ term. The order of the italic characters corresponds to the order of the greek characters (first position of the italic characters corresponds to first position of the greek characters, etc.). Although higher order basis functions can be included, we truncate the basis set at third order. From this basis set we are able to evaluate Eq. (8). The A_2 basis functions do not couple to any of the odd modes, unless we apply an external potential, and will be neglected. The A_3^3 basis functions do not couple to the A_1 basis set and will also be neglected. These approximations leave us with three types of basis functions, which we will label as $A_1\rightarrow a_1$, $A_3^1\rightarrow a_2$, $A_3^2\rightarrow a_3$. In the diffusion equation, Eq. (1), we redefine time to make thermal diffusion unity so that the adjoint diffusion operator becomes

$$
\mathbf{D}^{\dagger}=\sum_i\left[-\partial_{\theta_i}^2-\left(2J\sum_{j\neq i}\vec{u}_j'\cdot\mathbf{T}_{i,j}\cdot\vec{u}_i\right)\partial_{\theta_i}\right],
\tag{13}
$$

where $(\vec{u}_j')^{\alpha}=\partial_{\theta_j}\vec{u}_j^{\alpha}=\{-\sin(\theta_i),\cos(\theta_i)\}$. With these redefinitions, the adjoint operator acting on the a_1 basis functions gives

$$
\mathbf{D}^{+}(a_1)_i^{\alpha}=-(a_1)_i^{\alpha}-\sqrt{2}J\mathbf{T}_{ij}^{\alpha\xi}\vec{u}_j^{\xi}+\sqrt{2}J(\mathbf{B}_2)_i^{\alpha\xi}\mathbf{T}_{ij}^{\xi\nu}\vec{u}_j^{\nu}.
\tag{14}
$$

Summation is implied for all repeated indices and we introduce a matrix operator to simplify notation,

$$
(\mathbf{B}_m)_i=\begin{bmatrix}\cos(m\theta_i) & \sin(m\theta_i)\\ \sin(m\theta_i) & -\cos(m\theta_i)\end{bmatrix}.
\tag{15}
$$

It is important to note that the first number in $(\mathbf{B}_m)_i$ does not refer to an index. The product of $(\mathbf{B}_m)_i\vec{u}_i$ is a vector formed from a sum of products of $\{\cos(m\theta_i),\sin(m\theta_i)\}$ and can be decomposed into several elements of our basis set and should not be regarded as a single term.

A. A simple first order ansatz

The simplest approximation ignores the coupling to basis functions outside of the (a_1) class and the equilibrium contribution since these effects are small for small *J*. The lowest order truncation allows us to exactly diagonalize the diffusion operator within the basis set by defining Fourier modes,

$$
(\tilde{a}_1)_k^{\alpha}=\frac{1}{N}\sum_i\ \exp(-Ik\cdot i)(a_1)_i^{\alpha},
$$

where *N* is the length of the lattice, *I* is the imaginary number, and *i* refers the lattice position. The Green's function becomes

$$
\sum_{k,\alpha}|(\tilde{a}_1)_k^{\alpha}\rangle e^{-\lambda_k t}\langle(\tilde{a}_1)_k^{\alpha}|,
\tag{16}
$$

where $|\cdots\rangle$ and $\langle\cdots|$ represent the bra-ket structure and the eigenvalues, λ_k, have a simple form, $\lambda_k=-[1+2J(\cos(k_x)-\cos(k_y))]$. This expression shows a complex *k* vector dependence of the relaxation. The small *k* vector relaxation is similar to the relaxation predicted for free diffusion because the interaction is short ranged. For larger *k* vectors, the effects of the lattice structure on the relaxation become apparent. The relaxation in the *x* direction is faster than free diffusion while the relaxation in the *y* direction is slower. The favorable interaction for the $\cos(\theta_i)\cos(\theta_{i\pm(0)^1})$ results in faster relaxation for the *x* direction and the unfavorable interaction for $\cos(\theta_i)\cos(\theta_{i\pm(1)^0})$ results in the slower relaxation in the *y* direction. In the large lattice limit, $N\rightarrow\infty$, the single rotor orientation correlation function becomes

$$
\begin{aligned}
&\langle\cos(\theta_i(t))|\cos(\theta_i(0))\rangle\\
&\quad=\frac{1}{2}\int\frac{dk_x}{2\pi}\frac{dk_y}{2\pi}\exp[-t-2Jt\cos(k_x)\\
&\qquad+2Jt\cos(k_y)]\\
&\quad=e^{-t}I_0^2(2Jt),
\end{aligned}
\tag{17}
$$

where I_0 is the zeroth order Bessell function, and time is scaled so that $D_0=1$. The first order calculation is easily generalized to any bilinear potential with a well-defined discrete Fourier transform, by replacing the $\cos(k_{x,y})$ terms with the appropriate transfer matrix, which may mix the $\sin(\theta_i)$ and $\cos(\theta_i)$ basis sets. The result also extends to the three-dimensional case with the appropriate transfer matrix. As mentioned above, *J* is scaled by $\beta/2$ and time is scaled so that $D_0=1$.

In the long time limit, the orientation correlation function decays with an effective diffusion constant, $D_{\mathrm{eff}}=1-4J$. This result is reminiscent of the effective diffusion constant on rough energy surfaces derived by Zwanzig.[40] For weak interactions, there is no collective motions. Each rotor moves independently and the interactions simply impede the motion of the rotor, which slows down the overall rate of diffusion. The Bessell function comes from the integration over $\cos(k_x)$ and $\cos(k_y)$, which is similar to Zwanzig's prescription for calculating the effective diffusion constant,

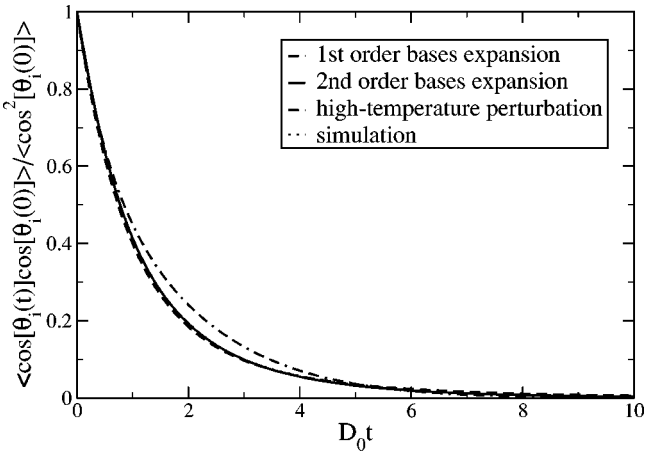

FIG. 1. $\langle \cos[\theta_i(t)]\cos[\theta_i(0)]\rangle$ autocorrelation function for $J=0.20$. Note that the high T direct perturbation result fails to fit the simulation even for this weak interaction, but the first order basis set has good agreement. The memory kernel result is not shown since it would be superimposed on the second order basis set result.

$$D_{\text{eff}}=D_0\cdot\left[\int\frac{d\theta}{2\pi}\exp(-\beta V(\theta))\right]\left[\int\frac{d\theta}{2\pi}\exp(+\beta V(\theta))\right], \tag{18}$$

with D_0 being the free diffusion constant.

Within the first order calculation, the relaxation of any k vector is given by exponential Debye behavior, but the relaxation of a single rotor, which is a sum of k vectors is non-Debye. The Debye behavior for first order comes from the simple Fourier diagonalization scheme that results in simple first order harmonic expressions for the relaxation of each mode. As the temperature is lowered, J increases, higher order effects explored below cause the spectrum of relaxation times to deviate from a monoexponential resulting in non-Debye behavior for the relaxation of a single dipole and each k vector component. These first order result are consistent with the finding of Berne that short range interactions do not lead to non-Debye behavior on long length scales, small k, but as will be shown below, more accurate calculations by incorporating higher order effects lead to non-Debye relaxation even for systems with nearest neighbor interactions.[30]

The first order result appears to be crude and the solution diverges at $J=0.25$, but the agreement with simulation is good for $J<0.20$. Figure 1 shows the good agreement, and Sec. IV discusses the reasons for the success of this simple first order ansatz. By inverting the diffusion operator and finding the eigenfunctions, even at this level of approximation, partially renormalizes the quantities, which improves the agreement by capturing the collective behaviors of the system. In the next section we elaborate on incorporating additional basis functions into our expansion, which allows us to achieve an exceptional fit to the simulation for $J=0.30$ and have a reasonable fit for $J=0.35$.

B. Higher order approximations to the Green's function

At the simplest level of approximation presented above, the basis set was easily diagonalized. For a more complicated higher order approximation, this is not necessarily the case, but we can still include effects from higher order basis set elements and achieve better agreement with simulation. To achieve this goal we determine the coupling between the basis elements presented in Eq. (12). The procedure produces an equation of the form, $\partial_t\vec{A}(t)=\mathcal{M}^T\vec{A}(t)$, where $\vec{A}(t)$ denotes the coefficients associated with these basis set elements, and the elements of the basis are denoted by omitting the time parameter t, and $\mathcal{M}^T$ is a matrix determined by the diffusion operator, $\mathcal{M}_{ij}=\langle\vec{A}_i|\mathbf{D}^\dagger\vec{A}_j\rangle$. The time parameter is omitted since we are referring to the basis functions. Note that the matrix is transposed since we are using the adjoint operator and the basis functions are real. The matrix $\mathcal{M}$ can be subdivided into submatrices $\mathcal{M}_{ij}$ that correspond to the overlap of elements of the a_i and a_j subsets of the basis functions,

$$\mathcal{M}=\begin{pmatrix}\mathcal{M}_{11}&\mathcal{M}_{12}&\mathcal{M}_{13}\\ \mathcal{M}_{21}&\mathcal{M}_{22}&\mathcal{M}_{23}\\ \mathcal{M}_{31}&\mathcal{M}_{32}&\mathcal{M}_{33}\end{pmatrix}. \tag{19}$$

It is difficult to find the eigenvectors of this matrix, even numerically. Approximately inverting the matrix is simpler so we take the Laplace transform of the equation, $t\to z$, and the propagator becomes $[\mathbf{I}z+\mathcal{M}^T]^{-1}$, with the identity operator $\mathbf{I}$, and Laplace variable z. From an arbitrary initial condition, $a_i(t=0)$, the value of the $a_1(t)$ basis functions at a future time is given by the inverse Laplace transform of

$$\begin{aligned}a_1(z)=&[\mathbf{I}z+\mathcal{M}^T]^{-1}_{11}a_1(t=0)+[\mathbf{I}z+\mathcal{M}^T]^{-1}_{12}a_2(t=0)\\&+[\mathbf{I}z+\mathcal{M}^T]^{-1}_{13}a_3(t=0),\end{aligned} \tag{20}$$

where $a_1(z)$ refers to the Laplace transform of the value of the coefficient associated with the a_1 basis set and $a_i(t=0)$ is the initial condition for these coefficients. We cannot exactly invert the matrix $[\mathbf{I}z+\mathcal{M}^T]$ so we must introduce some approximations. Our first order result corresponds approximating the off diagonal blocks in the first row of $[\mathbf{I}z+\mathcal{M}^T]$ as zero so that the values of the a_1 basis set are independent of the higher order basis set elements. Higher order approximations require more accurate forms for these matrix elements. The exact forms of the matrix elements of $\mathcal{M}_{ij}$ are presented in Appendix B. We can formally rewrite the $i1$ blocks of the inverse of the matrix $[\mathbf{I}z+\mathcal{M}]$ as

$$\begin{aligned}(\mathbf{I}z+\mathcal{M})^{-1}_{11}&=(\mathbf{I}z+\mathcal{M}'_{11})^{-1},\\(\mathbf{I}z+\mathcal{M})^{-1}_{21}&=(\mathbf{I}z+\mathcal{M}_{22})^{-1}\mathcal{M}_{23}(\mathbf{I}z+\mathcal{M}_{33})^{-1}\\&\quad\times\mathcal{M}_{31}(\mathbf{I}z+\mathcal{M}'_{11})^{-1},\\(\mathbf{I}z+\mathcal{M})^{-1}_{31}&=-(\mathbf{I}z+\mathcal{M}_{33})^{-1}\mathcal{M}_{31}(\mathbf{I}z+\mathcal{M}'_{11})^{-1},\end{aligned} \tag{21}$$

where

$$\mathcal{M}'_{11}=\mathcal{M}_{11}-\mathcal{M}_{13}(\mathbf{I}z+\mathcal{M}_{33})^{-1}\mathcal{M}_{31}+\mathcal{M}_{12}(\mathbf{I}z+\mathcal{M}_{22})^{-1}\mathcal{M}_{23}(\mathbf{I}z+\mathcal{M}_{33})^{-1}\mathcal{M}_{31}. \tag{22}$$

This result follows from solving the block matrix equations:

$$\begin{pmatrix} \mathbf{B}_{11} & \mathbf{B}_{12} & \mathbf{B}_{13} \\ \mathbf{B}_{21} & \mathbf{B}_{22} & \mathbf{B}_{23} \\ \mathbf{B}_{31} & \mathbf{B}_{32} & \mathbf{B}_{33} \end{pmatrix} \begin{pmatrix} \mathbf{A}_{11} & \mathbf{A}_{12} & \mathbf{A}_{13} \\ \mathbf{A}_{21} & \mathbf{A}_{22} & \mathbf{A}_{23} \\ \mathbf{A}_{31} & \mathbf{A}_{32} & \mathbf{A}_{33} \end{pmatrix} = \begin{pmatrix} \mathbf{I}_{11} & \mathbf{0}_{12} & \mathbf{0}_{13} \\ \mathbf{0}_{21} & \mathbf{I}_{22} & \mathbf{0}_{23} \\ \mathbf{0}_{31} & \mathbf{0}_{32} & \mathbf{I}_{33} \end{pmatrix}, \tag{23}$$

for each element $\mathbf{B}_{ij}$, where $\mathbf{I}_{ii}$ is an identity matrix for the sub-block and $\mathbf{0}_{ij}$ is a matrix of zeros. The simplified form follows from the elements of the $\mathcal{M}_{32}$ being identically zero.

It is important to note that we have calculated these quantities for the adjoint operator so the contributions to the propagation of the elements of the (a_1) basis set comes from the $(\mathbf{I}z+\mathcal{M})^{-1}_{i1}$ terms instead of the $(\mathbf{I}z+\mathcal{M})^{-1}_{1i}$ matrices that result from using the original diffusion operator. We only need to calculate these block matrices to determine the single spin autocorrelation function, but other matrices may be necessary to calculate higher order correlation functions. These equations are reminiscent of the results derived from the standard projection operator techniques, where the higher order effects of the dynamics become a nonexponential memory kernel. Up to this point the calculation is formally exact except for the truncation of the basis set to the elements of a_1, a_2, and a_3. For small values of J, the terms resulting from the diffusion operator $D_0\nabla^2_{\Omega_i}$ dominate the higher order basis functions, a_2 and a_3, and we can assume that they are approximately diagonal, $\mathcal{M}_{22}=(z+3)\mathbf{I}_{22}$, and $\mathcal{M}_{33}=(z+5)\mathbf{I}_{33}$. It is important to note that these assumptions do not capture all of the second order contributions, but the omitted second order contributions result in an expression that changes signs and give a partial cancellation—a random phase approximation. Under these assumptions, we evaluate the matrix elements of $(\mathbf{I}z+\mathcal{M})^{-1}_{l1}$. The form of the 11 block greatly simplifies

$$([\mathbf{I}z+\mathcal{M}'_{11}])^{\alpha\beta}_{ij}\approx\left(z+1+\frac{12J^2}{z+5}\right)\delta^{\alpha\beta}\delta_{ij}+J\left(1-\frac{12J^2}{(z+3)(z+5)}\right)(\mathbf{T})^{\alpha\beta}_{i,j}. \tag{24}$$

The Fourier transform introduced in Sec. III A also diagonalizes this matrix so the inverse can be calculated analytically although the inverse Laplace transform requires numerical calculation based on this analytic expression. It is important to note that this calculation, without considering other terms, already shows deviations from Debye behavior for every k vector even for this locally interacting model. This result is very different from the mean field calculations of Berne, which predicted that only long range interactions caused deviations from Debye theory in the small k limit.[30] The effects of translational motion on the relaxation was studied by Bagchi and Chandra and has been demonstrated to reduce if not eliminate non-Debye behavior in dipolar systems.[16] Berne's calculation also had translational motion although he did not analyze the interplay between translation and diffusion. The role of translation on non-Debye behavior in systems with short range interactions requires further investigation, but we expect that translation will have an even stronger effect on the non-Debye behavior of short range models.[16]

The other two blocks are easily expressed as products of the inverse of the 11 block expression in Eq. (24) with the coupling matrices,

$$[\mathbf{I}z+\mathcal{M}]^{-1}_{21}\approx\frac{1}{(z+3)(z+5)}\mathcal{M}_{23}\mathcal{M}_{31}[\mathbf{I}z+\mathcal{M}']^{-1}_{11},$$
$$[\mathbf{I}z+\mathcal{M}]^{-1}_{31}\approx\frac{1}{(z+5)}\mathcal{M}_{31}[\mathbf{I}z+\mathcal{M}']^{-1}. \tag{25}$$

The indexes are omitted, but follow the notation above. It is important to note that the inner product is over both the spinor variables (α,β) and the positions, $(i, j,$ etc.), but the $\sqrt{2}\cos(\theta_i)$ basis function and the $\sqrt{2}\sin(\theta_i)$ do not mix at any order of the expansion because symmetry prevents a preference for any directions. This result is related to the failure to form long range order for isotropic interactions in two-dimensions. The expressions in Eq. (24) and Eq. (25) are the approximate second order description of the dynamics that are needed to calculate the autocorrelation function for a single rotor, $\langle\cos(\theta_i(t))\cos(\theta_i(0))\rangle$. Because we neglect nearest neighbor interactions for the higher order basis functions, the Fourier modes in Sec. III A diagonalize this matrix. They need to be supplemented with the initial conditions, which are determined by the equilibrium distribution.

C. Equilibrium contribution

Although the basis set approach does not require the equilibrium initial condition, we will use the equilibrium so that we can compare our results to the standard GLE approach. The initial conditions are the result of evaluating the Boltzmann distribution,

$$\langle\chi(\{l''_i,m''_i,\Omega_i\})|\rho_{eq}(\{\Omega_i\})|\chi(\{l_i,m_i,\Omega_i\})\rangle. \tag{26}$$

The equilibrium distribution can be determined by finding the eigenfunction with zero eigenvalue, but as mentioned above, determination of the eigenfunctions and eigenvalues is difficult for a (infinitely) large matrix. Instead, we evaluate the equilibrium distribution perturbatively. The method follows the derivation of Rosenberg and Lax.[2,10,11,19] We perform a Taylor expansion of the canonical partition function and evaluate Eq. (26) term by term,

$$\rho_{\mathrm{eq}}=\eta\exp[-\beta V]=\eta(I-\beta V+\tfrac{1}{2}(\beta V)^2-\tfrac{1}{6}(\beta V)^3+\cdots), \tag{27}$$

where η is the normalization constant. Due to rotational symmetry and lack of long range order, the correlation of $\langle\rho_{\mathrm{eq}}(\{\theta_i\})\cos(\theta_i(0))^2\rangle=1/2$ for all interaction strengths, so we impose the normalization at the end of the calculation. The equilibrium contribution is calculated for terms that contribute up to second order in J. For interactions between

elements of the a_1 subset, the contributions come from the nearest neighbors and the next nearest neighbors,

$$\begin{aligned}
&\langle (a_1)_i^\alpha \rho_{\mathrm{eq}} (a_1)_i^\alpha \rangle = 1, \\
&\left\langle (a_1)_i^\alpha \rho_{\mathrm{eq}} (a_1)_{i\pm\binom{1}{0}}^\alpha \right\rangle = -J + \frac{J^3}{2}, \\
&\left\langle (a_1)_i^\alpha \rho_{\mathrm{eq}} (a_1)_{i\pm\binom{0}{1}}^\alpha \right\rangle = J - \frac{J^3}{2}, \\
&\left\langle (a_1)_i^\alpha \rho_{\mathrm{eq}} (a_1)_{i\pm 2\binom{1}{0}}^\alpha \right\rangle = J^2, \\
&\left\langle (a_1)_i^\alpha \rho_{\mathrm{eq}} (a_1)_{i\pm 2\binom{0}{1}}^\alpha \right\rangle = J^2, \\
&\left\langle (a_1)_i^\alpha \rho_{\mathrm{eq}} (a_1)_{i\pm\binom{0}{1}\pm(\mp)\binom{1}{0}}^\alpha \right\rangle = -2J^2.
\end{aligned} \tag{28}$$

The normalization for the autocorrelation functions is one because the basis functions are properly normalized, although $\int d\theta_i/(2\pi)\cos(\theta_i)^2 = 1/2$. We only need the equilibrium contribution to first order for the higher modes since their dynamics contribution is first order in J. These contributions are easily related to the dynamical parts calculated in Appendix B,

$$\begin{aligned}
\langle a_1 \rho_{\mathrm{eq}} a_3 \rangle &= -\tfrac{1}{2}\mathcal{M}_{12}, \\
\langle a_1 \rho_{\mathrm{eq}} a_3 \rangle &= -\tfrac{1}{3}\mathcal{M}_{13},
\end{aligned} \tag{29}$$

where $\mathcal{M}_{1i}$ are the matrices defined in Sec. III B and Appendix B.

Combining the dynamic and equilibrium parts gives the final expression for the Laplace transform of the single particle correlation function,

$$\begin{aligned}
\left\langle \rho_{\mathrm{eq}} a_{1,i} \frac{1}{z - D^+} a_{1,i} \right\rangle = {} & [\mathbf{I}z + \mathcal{M}'_{11}]^{-1}_{i,i} - 4J\left(1 - \frac{J^2}{2}\right)[\mathbf{I}z + \mathcal{M}'_{11}]^{-1}_{i+\binom{1}{0},i} + 4J^2[\mathbf{I}z + \mathcal{M}'_{11}]^{-1}_{i+2\binom{1}{0},i} - 8J^2[\mathbf{I}z + \mathcal{M}'_{11}]_{i+\binom{1}{1},i} \\
& + \frac{24J^3}{(z+3)(z+5)}[\mathbf{I}z + \mathcal{M}'_{11}]^{-1}_{i+\binom{1}{0},i} - \frac{4J^2}{(z+5)}[\mathbf{I}z + \mathcal{M}'_{11}]^{-1}_{i,i}.
\end{aligned} \tag{30}$$

In this expression, terms have been combined since elements of the matrix, such as $\mathcal{M}_{i,i\pm\binom{1}{0}}$, are related to other elements of the matrix, such as $\mathcal{M}_{i,i\pm\binom{0}{1}}$. The expression above can be evaluated to determine the single particle correlation function. As discussed previously, the Fourier modes diagonalize the matrix $[\mathbf{I}z + \mathcal{M}'_{11}]$ so the inverse can be done exactly, but the Laplace transform must be done numerically. These results are compared against a simulation and previous approaches to lattice dynamics in Sec. IV.

IV. COMPARISON WITH SIMULATION AND OTHER METHODS

We choose this simplified lattice system to allow comparison with very accurate Brownian dynamics simulations. The simulated system is a square lattice of rotors with periodic boundary conditions. For a given coupling strength, J, the length of each side of the lattice is increased by 4, until there is an agreement for three different lattice sizes. A lattice size of 40 is found to be sufficient for simulations with $J < 0.5$. This range of interaction strengths is below the Kosterlitz–Thouless phase transition temperature, $J < 0.55$, that has been examined extensively elsewhere, so finite size effects should be minimal.[36–38,41–43] Similarly, the time steps are adjusted by factors of 2^{-n} until there is an agreement between three consecutive time steps. Under the Brownian dynamics the system is allowed to equilibrate with a time determined by achieving agreement in the equilibrium correlation function of the lattice with random initial orientations and orientations in a single direction. The equilibration is also verified by performing Monte Carlo simulations to determine the equilibrium correlations and comparing them with the Brownian dynamics initial conditions.

The comparison of these simulations against the truncated basis expansion and the perturbation methods outlined in Appendix C are plotted for $J = 0.20$, 0.25, 0.30, and 0.35 in Figs. 1–4. In Figs. 1 and 2, the memory kernel expansion is omitted since it is close to our basis set solution. From these figures it is evident that the basis set approach matches the long time behavior of the simulation better than the other methods for all values of J. As mentioned in Sec. III A, for $J \leqslant 0.25$ even the simple ansatz is comparable to the other perturbation approaches. For $J > 0.25$ the Bessell function result predicted by the first order result in Eq. (17)

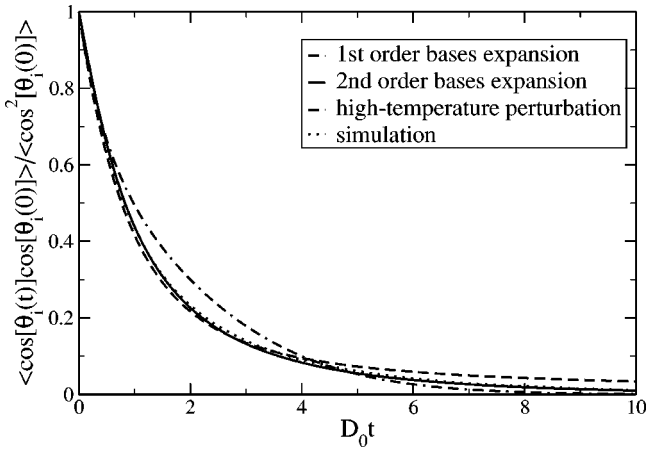

FIG. 2. $\langle \cos[\theta_i(t)]\cos[\theta_i(0)] \rangle$ autocorrelation function for $J = 0.25$. The first order result begins to break down, but the agreement between the second order result and the simulation is excellent. The memory kernel result is not shown since it would be super-imposed on the second order basis set result.

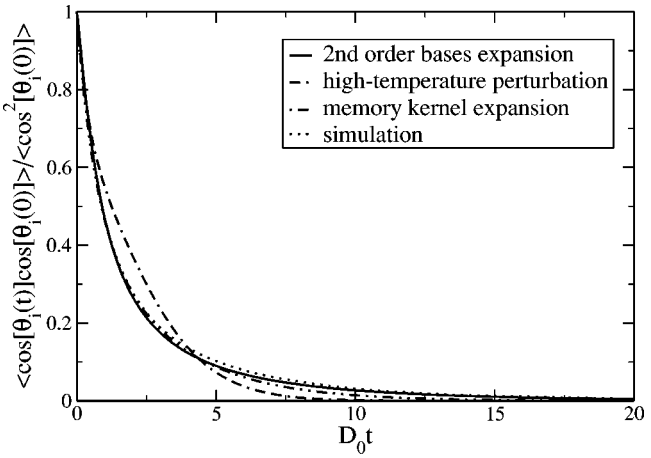

FIG. 3. $\langle \cos[\theta_i(t)]\cos[\theta_i(0)]\rangle$ autocorrelation function for $J=0.30$. In this figure, discrepancies between the memory kernel result becomes apparent in the long time regime.

outgrows the exponential term and the correlation function diverges. This prediction implies that the collective motions of the system are stronger than the dissipation of free diffusion. At this coupling strength, the system finds an additional mechanism for dissipation through coupling to higher basis functions. This result indicates that the higher order basis function become important at $J\approx 0.25$.

The second order basis set result incorporates these higher order contributions in the simplest form, an extra coupling between the first order basis set elements. These additional terms remove the divergence at $J=0.25$ and push the point where the coupling is stronger than the free diffusion to higher values of J. The simplified incorporation of these extra basis functions assumes that the elements of $\mathcal{M}_{23}$ and $\mathcal{M}_{32}$ are zero and the off diagonal elements of $\mathcal{M}_{22}$ and $\mathcal{M}_{33}$ are also zero. These off diagonal terms result in similar expressions to the one that diverges in the first order calculation. Although we do not present a full analysis, these divergences are canceled by coupling to higher order spherical harmonics, $\Sigma\, l_i > 5$.

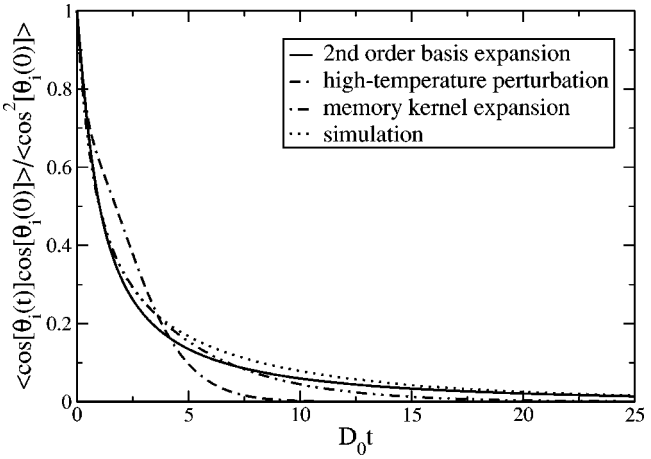

FIG. 4. $\langle \cos[\theta_i(t)]\cos[\theta_i(0)]\rangle$ autocorrelation function for $J=0.35$. In the short time the memory kernel expansion achieves good agreement with the simulation, but discrepancies between the memory kernel result become apparent in the long time regime. Conversely, the basis set expansion has good agreement at extremely short and long times, but deviates slightly for intermediate times.

The cause of the divergence for strong coupling is also the reason for the success of this basis set expansion. The divergence results from the basis expansion capturing the collective behaviors of the rotors. A perturbation expansion corresponds to only calculating the nearest neighbor interactions, which does not capture the entire collective motions. As a result, the perturbation expansion is always a multiexponential. The memory kernel expansion also includes interactions among basis functions in a perturbative manner that will always result in exponential long time relaxation. The memory kernel expansion captures the short time mean field dynamics since the equilibrium contribution is incorporated into the expansion, but it does not directly incorporate collective dynamics. This feature is very evident in Figs. 3 and 4. The memory kernel expansion does a better job than the basis set expansion at capturing the short time behavior since the equilibrium distribution is better approximated in this expansion, but the fit starts to deviate from the simulation curve for $t>6$. In contrast, the basis set deviates slightly from the simulation for intermediate times, but the calculation starts to fit the simulation data very well for longer times.

The agreement for short times is the result of the coupling between basis functions being retarded, so that the initial process corresponds to diffusion in a mean field environment that is not correlated to the motion of the rotor. Since we incorporate the equilibrium distribution, the shape of the potential energy surface at $t=0$ is approximately correct resulting in the proper equation of motion. At intermediate times, the collective motions begin to play a role causing deviations from the behavior predicted by the basis set calculation. The two contributions to the collective behavior come from coupling between the first order basis set and coupling between the higher order basis sets. We treat the first order basis sets exactly, so that we get the contributions from their coupling correct. The contributions from higher order basis sets are treated approximately, but since the free diffusion term causes these contributions to decay faster than the contributions from the first order basis set, these higher order contributions become small at long times and better agreement at longer times is achieved. The memory kernel expansion captures the dynamics in the initial time by incorporating the correct mean field results, but it does not completely capture the collective behaviors that are important at longer times. (See Fig. 5.)

As the interaction strength, J, increases, the collective motions of the rotors become more important causing a slow down in the overall relaxation. The slow down of the relaxation time is demonstrated in Fig. 6. As can be seen from Fig. 6, the relaxation time is a strong function of J. The calculated relaxation time is in good agreement with the simulation, but the calculation systematically underestimates the relaxation time. The calculation predicts a divergence in the relaxation time at $J=0.38$. Considering the predicted KT phase transition at $J\approx 0.55$ discussed below (Sec. V) and the power-law behavior of the simulation at $J=1.0$, the diver-

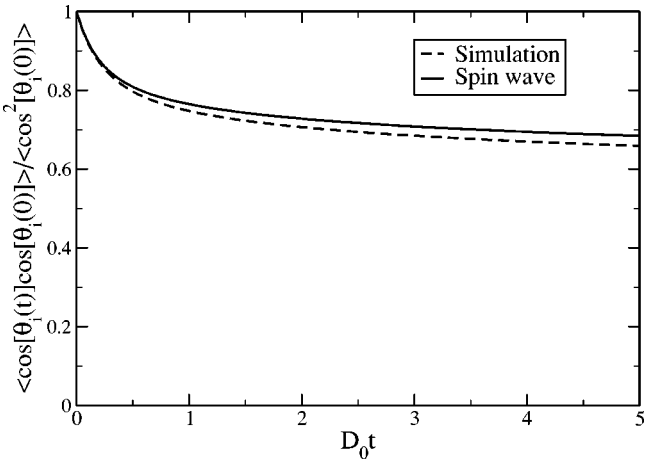

FIG. 5. The behavior of $\langle \cos[\theta_i(t)]\cos[\theta_i(0)]\rangle$ for $J=1.0$. The low temperature regime requires collective spin-wave modes. The spin-wave captures the correct initial decay since the potential is approximately harmonic and the spin-wave solution agrees with the long time power law. The deviation in the intermediate time is caused by the potential not being perfectly harmonic. The simulation has a slight finite size effect that causes some uncertainty in the power-law exponent of the simulation.

gence is expected for the system although the position of the divergence is difficult to determine from the simulation. The strong dependence on J comes from the increasing importance of larger clusters of spins. Eventually, all orders of the single rotor basis functions are necessary to capture the collective motions on long time scales, but the short time still depends on the motions of individual rotors in a mean field potential and is captured by this basis set, as long as the proper zero time correlations are incorporated. Capturing longer time collective behavior requires the introduction of another basis, such as the spin-wave basis. In Sec. V, we discuss the role of spin-wave modes for long time behavior. We also relate these considerations to similar results found in Langevin dynamics and mode-coupling theory.

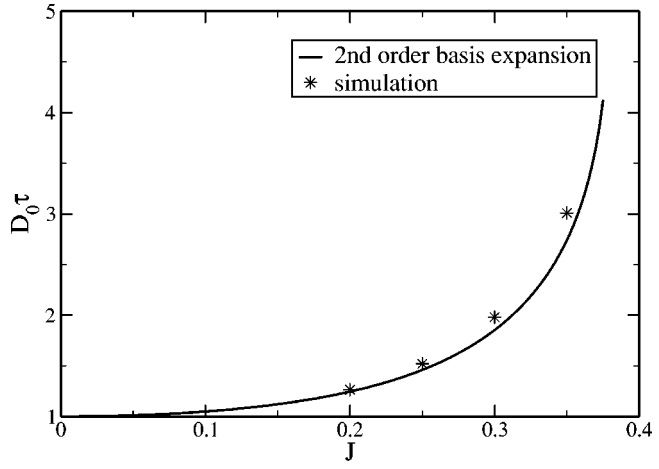

FIG. 6. The mean relaxation time of a single rotor as a function of J. The relaxation time is a strong function of J because of the increasing importance of collective motions.

V. LOW TEMPERATURE PHASE

As discussed above, this system can be mapped onto the plane rotor model that has been extensively studied in the field of high temperature superconducting physics.[36–38] If we apply the mapping outlined in Sec. I $[(\theta_{2i}\rightarrow\theta_{2i}),\ (\theta_{2i+\binom{1}{0}}\rightarrow-\theta_{2i+\binom{1}{0}}),\ (\theta_{2i+\binom{1}{0}}\rightarrow\pi-\theta_{2i+\binom{0}{1}})$, and $(\theta_{2i+\binom{1}{1}}\rightarrow\theta_{2i+\binom{1}{1}}-\pi)]$, the potential becomes

$$\beta V(\{\theta_i\})=-2J\sum_i \cos(\theta_i-\theta_j)(\delta_{i+\binom{1}{0}}+\delta_{i+\binom{0}{1}}). \quad (31)$$

The low temperature phase of this system possesses the exotic Kosterlitz–Thouless phase transition, where the system fails to achieve long-range order at a finite temperature, but the distance dependence of the correlation between orientations of rotor is a power law.[36–38,41–43] Although discrepancies in simulations exist, the phase transition occurs around $0.85<(\beta V)^{-1}<0.95$, where β is the inverse temperature. This temperature corresponds to $J\approx 0.55$, which is above the region that our basis set expansion is accurate so we introduce a spin-wave basis set that captures the collective modes of the system at low T.

The harmonic basis set expansion is applied to $J=1.0$. The simulation is the same as the high temperature simulations, but a slightly larger lattice of 52×52 was required, and some size effects are still present even for this lattice. A comparison of the simulation and the spin-wave solution is presented in Fig. 5. At low temperatures, a single rotor spends most of its time in the bottom of the well formed by the interactions with its neighbors. Due to the periodic nature of this potential with only a single minimum, even if the rotor hops over the barrier, it returns to the well from the other side. As a result, the movement of a single rotor is not important for long time behavior. The important motion on long time scales is the diffusion of the well, which is a collective motion that depends on the movement of the neighbors. We make a harmonic approximation for the well with a single force constant κ. The potential becomes $-2J\cos(\theta_i-\theta_j)\approx-\text{const}+(1/2)\kappa(\theta_i-\theta_j)^2$. Mean field variational arguments determines that the force constant of the harmonic pseudopotential is given by the expression found in a reference, $\kappa=2J\exp(-1/(4\kappa))$.[41] For $J<0.34=J_c$, the only solution to this equation is $\kappa=0$. For $J\geqslant J_c$, κ initially grows as $(J-J_c)^{1/2}$. For large $J\gg0.34$, κ approaches the value of J as a power law, $(\kappa/2J)\rightarrow1-\frac{1}{8}J^{-1}+O(J^{-2})$. This behavior is common for mean field solutions.

Standard analysis gives the Green's function for the motions of the harmonic modes of the system (spin waves), $\theta_k=(1/N)\Sigma_j\exp[Ik\cdot j]\theta_j$. The $\langle\cos(\theta_i(t))\cos(\theta_i(0))\rangle$ correlation function becomes a result of simple Gaussian integrals,

$$\langle\cos(\theta_i(t))\cos(\theta_i(0))\rangle = \frac{1}{2}\exp\left(-2\int_0^{D_0t}dt'\,\exp(-2d\kappa t')I_0^d(2\kappa t')\right), \quad (32)$$

where d is the dimension of the lattice. For $d=2$ the integral in the exponential resembles the first order basis set result.

Since the Bessell function, $I_0(t)$, behaves as $(1/\sqrt{2\pi t})e^t$ for large values of t, we can approximate $-2\int_0^{D_0 t} dt'\, I_0^2(2\kappa t')e^{-2(2\kappa)t'}$ as $\text{const}+-2\int_{D_0 t_0}^{D_0 t} dt' \times[1/2\pi(2\kappa)t'] = \text{const}-(1/2\pi\kappa)\ln(D_0 t')$. In this expression t_0 is a time where the approximation becomes valid. Since the log is in the exponential, the resulting expression for the correlation decay is a power law with a small exponent of $(2\pi\kappa)^{-1}$. This power-law decay is expected for a strongly coupled system, and can be understood through an analogy with Goldstone modes. As the k vector of the normal modes goes to zero, the force constant of the modes, i.e., density of states, also goes to zero and at any time scale there is always a slow component, which results in the power law. Interestingly, for $d \geqslant 3$ the integral is finite and the correlation function does not decay to zero. For $d=1$, the long time behavior of the integral is $t^{1/2}$ and the system behaves as a stretched exponential. The stretched exponential occurs naturally in this calculation and demonstrates the role of the density of states around zero in determining the long time functional form. In analogy to thermodynamics, three is the critical dimension.

As seen in Fig. 5, similar to the results with the high temperature basis set, the spin-wave approximation captures the short time behavior fairly well since the potential is approximately harmonic. For intermediate times there is a slight discrepancy between the behaviors of the two systems. This effect is a result of the potential being not truly harmonic and allows additional relaxation through defects which is similar to defect mediated melting in the KT phase transition.[36–38,41–43] The simulation and the spin-wave solution behave as power laws in the long time limit with similar exponents. The exponent is 0.065 for the spin wave versus the simulation result, which is approximately 0.072. Although the defect relaxation mechanisms that are not captured by the spin wave may cause the discrepancies, a finite size effect causes uncertainty in the simulation exponent so the spin-wave prediction is well within the error in the measurement of the simulation result for low temperature.

Considering that both the simulation and the spin-wave calculation behave as similar power laws in the long time limit, the spin-wave basis set appears to capture the fundamental long time relaxation mechanisms of this system. The deviations occur during intermediate times before the system enters into the power law. From this point of view, the error in the calculation appears to be caused by a weighting between short time components of the relaxation and the long time power-law components. The spin wave simply overestimates coefficient of the power-law contribution to the relaxation.

The failure to capture intermediate time correlations, but the success at capturing both short and long time behaviors can be understood through barrier hopping. The short time agreement is caused by intrawell relaxation that is captured by the harmonic potential. The deviation at intermediate times is caused by a barrier hopping mechanism. For the harmonic potential, the system can only relax by sliding down the sides of the well, but the real system has the ability to jump over the barrier to the other side, which adds an additional relaxation mechanism that occurs at intermediate times. As the temperature is lowered, the importance of the hopping mechanism will reduce. The hopping causes a loss of correlations, which reduces the overall height of the correlation function as it enters into the power-law regime. This loss is not captured by the spin wave. However, barrier hopping is not as important as expected for a single well periodic potential since the particle will enter the well on the other side. As discussed above, it is the diffusion of the well itself that dominates the long time relaxation. Since the well is formed by four nearest neighbors, the relaxation of the well is determined by collective motions. The time separation of single particle intrawell relaxation and the collective relaxation of the wells makes the harmonic approximation of this long time relaxation accurate, which results in the agreement of the power-law exponents.

VI. CONCLUDING REMARKS

In this paper we examined a two-dimensional rotor model with local interactions. By using different truncated basis sets, we are able to capture the behavior of this system in both the high temperature and low temperature regimes. For very high temperature, the rotors act independently, but their interactions hinder each other. This results in long time Debye relaxation with a reduced diffusion constant. For stronger interactions, the rotors begin to show collective motions, which results in strongly non-Debye behavior. At lower temperatures, the system behaves as a spin-wave system with long time power-law relaxation.

As demonstrated for this simple planar rotor model, generalized Langevin dynamics can be applied in various forms. The basic requirement is the ability to approximately remove some degrees of freedom by introducing a memory kernel. The standard approach to deriving the GLE is with projection operator methods that use a specific projection operator (or inner-product). These projection operator approaches have been successfully used in many applications. One difficulty with the standard projection operators is the restriction on the basis elements and the incorporation of the equilibrium distribution in the inner-product of the space. If the rotor orientation is the desired quantity of interest, practical implementations of the standard projection operator approach restricts the basis set to one that contains the single rotor orientation. The basis set of individual rotors is not orthogonal with respect to the equilibrium weighted inner-product, and applying the Gram–Schmidt procedure is necessary, which can make the equations complicated and obscure the physics.

Another approach to generalized Langevin dynamics is a basis set approach. In this approach, we choose the basis set and then define the desired quantities in terms of overlaps of the basis set elements. Different basis sets may have an advantage over other basis sets as shown by the spin-wave fit in the low temperature and long time versus the single particle basis set in the high temperature and short time. This approach is also a projection operator technique, but the projection is with respect to the basis set instead of the measured degree of freedom with an equilibrium weighted inner-product. In this approach the projection operator is tempera-

ture and interaction independent. One can easily perform transformation on this basis set, like the Fourier transform performed in Sec. III A. This truncation is independent of the equilibrium distribution, which may be useful in studying systems far from equilibrium. The basis set has the ability to capture collective motions that are omitted in the standard projection operator approaches, which is important in different applications.

The two approaches to deriving generalized Langevin dynamics are complementary, as are different basis sets, and should be used together to determine various properties of the system. The standard projection operator approach accurately captures the many-body equilibrium effects while the truncated basis set approach captures collective motions directly. These two strengths will be combined in future studies of these Brownian dynamic systems. The inner-product space, which defines the projection operator, should be chosen to reveal the desired physics. As is standard in linear algebra, proper choices of basis sets make computation easier. The basis set approach is used to determine the properties of the facilitated kinetic Ising model in a companion paper.[34] Future work extends this approach to a dipolar system that is similar to the original model studied by Zwanzig, but where disorder in the particle positions is introduced.[1,2]

ACKNOWLEDGMENTS

This research is supported by the AT&T Research Fund Award, the NSF Career Award (No. Che-0093210) Camille Dreyfus Teacher-Scholar Award, and Petroleum Research Fund.

APPENDIX A: THE BASIS SET AND GLE

The standard derivation of the GLE equation for many-particle dynamics follows the Zwanzig–Mori projection operator formalism. The general spirit of projection operator methods is to separate the dynamics into different contributions, which can then be approximated through various techniques. The equations after the application of the projection operator are exact, but the approximations required to evaluate expressions will differ with different projection operators. Because the initial equations are exact, all projection operator methods are formally equivalent. The benefits and disadvantages of using different projection operators will depend on the application. Hynes and Deutch discuss various classes of projection operators and when these operators are generally applied.[44] Generally, using different projection operators correspond to different representations of the same dynamics.

The quantities that we measure correspond to the elements of the basis set A_1 defined above. The projection operators $\mathbf{P}$ and $\mathbf{Q}$ are traditionally defined as $\mathbf{P}=|A_1\rangle\mathbf{K}_{11}^{-1}\langle A_1|$ and $\mathbf{Q}=\mathbf{I}-\mathbf{P}$. The matrix $\mathbf{K}_{11}$ is the matrix elements that result from the inner product of the elements of the A_1 basis set, $\mathbf{K}_{11}=\langle A_1|A_1\rangle$. The standard GLE approach defines this inner-product as $\langle A|B\rangle=\int d\Gamma\, A^{\dagger}B\rho_{\mathrm{eq}}$. In this expression for the inner-product, $d\Gamma$ denotes integration over the phase space and ρ_{eq} is a weighting by the equilibrium distribution. This definition is not necessary and results in a complicated expression for $\mathbf{K}_{11}$ and forces us to use Gram–Schmidt to construct an orthogonal basis set,

$$\begin{aligned} Q_1&=A_1,\\ Q_2&=A_2-\langle\rho_{\mathrm{eq}}A_2Q_1\rangle\langle\rho_{\mathrm{eq}}Q_1Q_1\rangle^{-1}Q_1,\\ Q_3&=A_3-\langle\rho_{\mathrm{eq}}A_3Q_1\rangle\langle\rho_{\mathrm{eq}}Q_1Q_1\rangle^{-1}Q_1\\ &\quad-\langle\rho_{\mathrm{eq}}A_3Q_2\rangle\langle\rho_{\mathrm{eq}}Q_2Q_2\rangle^{-1}Q_2,\\ &\cdots. \end{aligned} \tag{A1}$$

The equilibrium weighted inner-product must be evaluated with perturbation methods, and the equilibrium distribution appears in many places in the expression, unlike the inclusion in the initial condition in the basis set approach. Many of these terms cancel, but the algebra is increased greatly. This expansion makes the basis set elements complicated functions of the perturbation parameter. As a result, one does not necessarily achieve higher accuracy by including the equilibrium distribution in the inner-product.

The complications caused by the equilibrium distribution can be avoided by using an unweighted inner product. At each order in the expansion, the resulting equation is equivalent to the standard GLE since the two expansions only differ by higher order terms. The GLE can be calculated from the basis set approach resulting in the expression

$$\dot{C}(t)=\langle\dot{A}_1(t)A_1(0)\rangle=-\Omega C(t)-\int_0^t M(t-\tau)C(\tau)d\tau, \tag{A2}$$

where Ω is the decay rate, $\Omega=\langle A_1|\mathbf{D}|A_1\rangle\mathbf{K}_{11}^{-1}$, and $M(t)$ is the memory kernel, $M(t)=\langle f(t)|f(t)\rangle K_{11}^{-1}$. The memory kernel's Laplace transform can be easily expressed in the basis set notation $M(z)=\mathcal{M}_{12}\hat{C}_2(z)\mathcal{M}_{12}$, with

$$\hat{C}_2(z)=[z\mathcal{I}-\mathcal{M}_{22}-\mathcal{M}_{23}(z\mathcal{I}-\mathcal{M}_{33}-\cdots)^{-1}\mathcal{M}_{23}]^{-1}. \tag{A3}$$

The expression for $\hat{C}_2(z)$ is the result of Mori's continued fraction.

The projection operators are constructed from the definition of the inner-products. To any order in the perturbation expansion, the projection operators will be equivalent, but for some many-particle systems such as this problem, excluding the equilibrium distribution from the definition of the projection operator brings benefits by separating kinetic and equilibrium effects, making the projection operator independent of the order of the perturbation expansion, and allowing one to naturally change basis sets to measure different effects, such as single particle properties versus Fourier modes.

APPENDIX B: MATRIX ELEMENTS FOR TRUNCATED BASIS SET EXPANSION

The matrix elements of the truncated basis set expansion are calculated by applying the adjoint diffusion operator to the basis set element and taking the inner-product of this expression with the other elements of the basis set. In these expressions, the basis set elements will once again be in tensor form, with α, β, and γ and i, j, k referring to the row

of the matrix element and ξ, η, and ν and p, q, and r referring to the column. Other variables that appear in the expressions are dummy values that are summed over. We also introduce a permutation operator, $\mathbf{P}_{ijk}^{\alpha\beta\gamma}$, which implies that the permutation of all variables must be taken. Italic characters still refer to lattice position and greek characters refer to $\cos(\theta_i)$ or $\sin(\theta_i)$. Also following previous notation, the order of the italic characters corresponds to the order of the greek characters so that the expressions are similar to

$$(\mathcal{M}_{22})_{ijkpqr}^{\alpha\beta\gamma\xi\eta\nu}=\langle(a_2)_{ijk}^{\alpha\beta\gamma}|\mathbf{D}^{\dagger}(a_2)_{pqr}^{\xi\eta\nu}\rangle. \tag{B1}$$

We used the fact that the basis set is real to exchange the order in the inner-product. With this notation, the matrix elements become the overlap of $\mathbf{D}^{\dagger}(a_1)_i^{\alpha}$ with the other basis elements,

$$\begin{aligned}
(\mathcal{M}_{11})_{ip}^{\alpha\xi}&=\langle(a_1)_i^{\alpha}|\mathbf{D}^{\dagger}(a_1)_p^{\xi}\rangle=\delta^{\alpha\xi}\delta_{ip}+J\mathbf{T}_{ip}^{\alpha\xi},\\
(\mathcal{M}_{21})_{ijkp}^{\alpha\beta\gamma\xi}&=\langle(a_2)_{ijk}^{\alpha\beta\gamma}|\mathbf{D}^{\dagger}(a_1)_p^{\xi}\rangle=0,\\
(\mathcal{M}_{31})_{ijq}^{\alpha\beta\xi}&=\langle(a_3)_{ij}^{\alpha\beta}|\mathbf{D}^{\dagger}(a_1)_p^{\xi}\rangle\\
&=-\sqrt{2}J\langle u_p^{\xi}|(\mathbf{B}_2)_i^{\alpha\lambda}\rangle\mathbf{T}_{iq}^{\lambda\eta}\delta_{ip}.
\end{aligned} \tag{B2}$$

In the above expression, the dummy index, λ, is summed over to give the final expression and the inner-products refer to a matrix that is determined by the element by element inner-product. Note the tensor form of the expressions, which is consistent with the formalism presented above with δ_{ip} and $\delta^{\alpha\xi}$ being Kronecker-δ functions.

We get a similar expression for the overlap of the $\mathbf{D}^{\dagger}(a_2)$ basis elements,

$$\begin{aligned}
(\mathcal{M}_{12})_{ipq}^{\alpha\xi\eta}&=\langle(a_1)_i^{\alpha}|\mathbf{D}^{\dagger}(a_2)_{pqr}^{\xi\eta\nu}\rangle=J\sum_{\mathbf{P}_{pqr}^{\xi\eta\nu}}\mathbf{T}_{pq}^{\xi\eta}\delta^{\alpha\gamma}\delta_{ir},\\
(\mathcal{M}_{22})_{ijkpqr}^{\alpha\beta\gamma\xi\eta\nu}&=\langle(a_2)_{ijk}^{\alpha\beta\gamma}|\mathbf{D}^{\dagger}(a_2)_{pqr}^{\xi\eta\nu}\rangle\\
&=\sum_{\mathbf{P}_{ijk}^{\alpha\beta\gamma},\mathbf{P}_{pqr}^{\xi\eta\nu}}\delta^{\alpha\xi}\delta_{ip}\delta^{\beta\eta}\delta_{jq}\delta^{\gamma\nu}\delta_{kr}\\
&\quad+J/2\mathbf{T}_{ip}^{\alpha\xi}\delta^{\beta\eta}\delta_{jq}\delta^{\gamma\nu}\delta_{kr},\\
(\mathcal{M}_{32})_{ijpqr}^{\alpha\beta\xi\eta\nu}&=\langle(a_3)_{ij}^{\alpha\beta}|\mathbf{D}^{\dagger}(a_2)_{pqr}^{\xi\eta\nu}\rangle=0.
\end{aligned} \tag{B3}$$

It is important to note that $(p>q>r)$ is part of the definition of the elements of the (a_2) basis functions so that the permutation gives $\exp(-3t)$ for free diffusion.

The final overlap matrices that we must calculate is for the $\mathbf{D}^{\dagger}(a_3)$ terms,

$$\begin{aligned}
(\mathcal{M}_{13})_{ipq}^{\alpha\xi\eta}&=\langle(a_1)_i^{\alpha}|\mathbf{D}^{\dagger}(a_3)_{pq}^{\xi\eta}\rangle\\
&=3\sqrt{2}J\langle u_i^{\alpha}(\mathbf{B}_1')_p^{\xi\lambda}\rangle\mathbf{T}_{pq}^{\lambda\eta}\delta_{ip},\\
(\mathcal{M}_{23})_{ijkpq}^{\alpha\beta\gamma\xi\eta}&=\langle(a_2)_{ijk}^{\alpha\beta\gamma}|\mathbf{D}^{\dagger}(a_3)_{pq}^{\xi\eta}\rangle\\
&=2^{3/2}J\sum_{\mathbf{P}_{ijk}^{\alpha\beta\gamma}}\langle u_i^{\alpha}(\mathbf{B}_1')_p^{\xi\lambda}\rangle\mathbf{T}_{p,k}^{\lambda\beta}\delta^{\gamma\eta}\delta_{kp},\\
(\mathcal{M}_{33})_{ijpq}^{\alpha\beta\xi\eta}&=\langle(a_3)_{ij}^{\alpha\beta}|\mathbf{D}^{\dagger}(a_3)_{pq}^{\xi\eta}\rangle\\
&=5\delta^{\alpha\xi}\delta_{ip}\delta^{\beta\eta}\delta_{jq}+J\mathbf{T}_{jq}^{\beta\eta}\delta^{\alpha\xi}\delta_{ip}\\
&\quad+2J\langle\vec{u}_{2i}^{\alpha}(\mathbf{B}_2)_q^{\lambda\eta}\rangle\mathbf{T}_{pq}^{\lambda\zeta}\langle\vec{u}_j^{\beta}(\mathbf{B}_1')_p^{\xi\zeta}\rangle,
\end{aligned} \tag{B4}$$

where

$$(\mathbf{B}_m')_i=\begin{bmatrix}\cos(m\theta_i) & -\sin(m\theta_i)\\ \sin(m\theta_i) & \cos(m\theta_i)\end{bmatrix}, \tag{B5}$$

has a similar definition as $(\mathbf{B}_m)_i$ above. The dummy variables λ and ζ are summed over all arguments. From these expressions we are able to approximately determine the matrix elements in Eq. (8), which allows us to calculate the dynamics of the system.

APPENDIX C: DIRECT PERTURBATION AND MEMORY KERNEL PERTURBATION EXPANSION

Figures 1–4 compare our truncated basis set expansion with other perturbation methods that have been previously used to study similar lattice systems. In this appendix, we outline two alternative approaches and give the expressions that result from these methods.

1. Direct perturbation

The direct perturbation approach has been successfully used to study the Brownian dipolar lattice.[1,2] This method is easily understood by Laplace transforming the equation

$$\begin{aligned}
C_{ij}^{\alpha\beta}(z)&=\langle\rho_{\mathrm{eq}}\vec{u}_i^{\alpha}[\mathbf{I}z-\mathbf{D}^{\dagger}]^{-1}\vec{u}_j^{\beta}\rangle=\langle\rho_{\mathrm{eq}}\vec{u}_i^{\alpha}[\mathbf{I}z-\mathbf{D}_0^{\dagger}]^{-1}\vec{u}_j^{\beta}\rangle+\langle\rho_{\mathrm{eq}}\vec{u}_i^{\alpha}[\mathbf{I}z-\mathbf{D}_0^{\dagger}]^{-1}\mathbf{D}_1^{\dagger}[\mathbf{I}z-\mathbf{D}_0^{\dagger}]^{-1}\vec{u}_j^{\beta}\rangle\\
&\quad+\langle\rho_{\mathrm{eq}}(\{\theta_i\})\vec{u}_i^{\alpha}[\mathbf{I}z-\mathbf{D}_0^{\dagger}]^{-1}\mathbf{D}_1^{\dagger}[\mathbf{I}z-\mathbf{D}_0^{\dagger}]^{-1}\mathbf{D}_1^{\dagger}[\mathbf{I}z-\mathbf{D}_0^{\dagger}]^{-1}\vec{u}_j^{\beta}\rangle+\cdots.
\end{aligned} \tag{C1}$$

Similar to above, $\mathbf{D}_0^{\dagger}$ is the free diffusion operator and $\mathbf{D}_1^{\dagger}$ is the term that comes from the interactions, Eq. (2). The equilibrium contribution, $\rho_{\mathrm{eq}}(\{\theta_i\})$ is determined using the same method we use in Sec. III C. This expansion can be easily calculated up to second order, as well as inverted into the time domain. The resulting expression for $D_0=1$ is

$$\begin{aligned}
C_{ii}^{\alpha\alpha}(t)&\approx(1-J^2/2)\exp[-t]+2J^2t\exp[-t]\\
&\quad+4J^2t^2\exp[-t]+J^2/2\exp[-5t].
\end{aligned} \tag{C2}$$

As we can see, this expression is a simple sum of polynomials multiplying exponentials, which does not reflect the complex behavior of our simple system for modest values of J.

2. Memory kernel expansion

The memory kernel expansion approach has also been used to study the dipolar lattice.[10,11] This expansion starts from the Zwanzig–Mori projection formalism,

$$C_{ij}^{\alpha\beta}(z)=\langle\rho_{\mathrm{eq}}(\{\Omega_i\})\vec{u}_i^{\alpha}[\mathbf{I}z-\mathbf{D}^{\dagger}]^{-1}\vec{u}_j^{\beta}\rangle$$
$$=[z\mathbf{I}+\mathbf{\Lambda}-\mathbf{M}]^{-1}\mathbf{G} \tag{C3}$$

with

$$\mathbf{G}_{ij}^{\alpha\beta}=\langle\vec{u}_i^{\alpha}|\rho_{\mathrm{eq}}(\{\Omega_i\})|\vec{u}_j^{\beta}\rangle,$$

$$\mathbf{\Lambda}_{ij}^{\alpha\beta}=-\sum_{k,\gamma}\langle\rho_{\mathrm{eq}}(\{\Omega_i\})\vec{u}_i^{\alpha}|\mathbf{D}^{\dagger}\vec{u}_k^{\gamma}\rangle(\mathbf{G}^{-1})_{kj}^{\gamma\beta}, \tag{C4}$$

$$(\mathbf{M})_{ij}^{\alpha\beta}=\sum_{k,\gamma}\langle\rho_{\mathrm{eq}}(\{\Omega_i\})\vec{u}_i^{\alpha}|\mathbf{D}^{\dagger}\mathbf{Q}[\mathbf{I}z-\mathbf{D}^{\dagger}\mathbf{Q}]^{-1}\mathbf{Q}\mathbf{D}^{\dagger}\vec{u}_k^{\gamma}\rangle$$
$$\times(\mathbf{G}^{-1})_{kj}^{\gamma\beta},$$

where $\mathbf{Q}=\mathbf{I}-|\vec{u}\rangle\mathbf{G}^{-1}\langle\rho_{\mathrm{eq}}(\{\Omega_i\})\vec{u}|$ is our standard projection operator. In the above notation, we dropped the indexes that are summed over in this matrix representation except for the γ and k, since these appear on a dipole vector, $\vec{u}$. The matrix $\mathbf{M}$ corresponds to the memory kernel in mode-coupling theory and $\mathbf{\Lambda}$ corresponds to the eigenfrequency. The $\mathbf{G}$ is the equilibrium correlation function that we calculated in Sec. III C and $[\mathbf{I}z-\mathbf{\Lambda}-\mathbf{M}]^{-1}$ is the mode-coupling analogue of the dynamic portion of our calculation.

We perturbatively expand $\mathbf{G}$, $\mathbf{\Lambda}$, and $\mathbf{K}$ in terms of J to second order, which gives

$$([\mathbf{I}z-\mathbf{\Lambda}-\mathbf{M}]^{-1}\mathbf{G})_{ii}^{\alpha\alpha}\approx\frac{1}{2}\frac{1}{(z+1)-\dfrac{4J^2}{z+1}-\dfrac{4J^2}{z+5}}. \tag{C5}$$

This expression includes all second order contributions, unlike our simple approximation that only captures some of the second order contributions. The $(z+1)$ term comes from free diffusion. Similar to Zwanzig's perturbation expansion, the $(z+1)^{-1}$ term comes from coupling of the $\vec{u}_i^{\alpha}$ to its neighbors and the $(z+5)^{-1}$ term comes from coupling to the basis functions that are in the a_3 subset of our truncated basis set expansion (although the expansion does not explicitly include this basis set). This result along with the direct perturbation result and our truncated basis set calculation are presented in Figs. 3 and 4. As mentioned in Sec. IV, the memory kernel expansion captures the initial many-body effects and accurately describes the system at short time, but is not as accurate at capturing longer time behavior as the basis set approach at the same order of expansion. So these two approaches are to be viewed as complementary.

[1] T. W. Nee and R. Zwanzig, J. Chem. Phys. **52**, 6353 (1970).
[2] R. Zwanzig, J. Chem. Phys. **38**, 2766 (1963).
[3] R. A. Marcus, Rev. Mod. Phys. **65**, 599 (1993).
[4] Y. Tanimura, V. B. P. Leite, and J. N. Onuchic, J. Chem. Phys. **117**, 2172 (2002).
[5] P. Kedziora, J. Jadzyn, and L. Hellemans, Phys. Rev. E **66**, 031702 (2002).
[6] L. A. Deschenes and D. A. V. Bout, Science **292**, 255 (2001).
[7] R. D. Deegan, R. L. Leheny, N. Menon, and S. R. Nagel, J. Phys. Chem. B **103**, 4066 (1999).
[8] C. A. Angell, B. E. Richards, and V. Velikov, J. Phys.: Condens. Matter **11**, A75 (1999).
[9] L. Brennan, D. L. Turner, P. Fareleira *et al.*, J. Mol. Spectrosc. **208**, 353 (2001).
[10] H. Z. Zhou and B. Bagchi, J. Chem. Phys. **97**, 9311 (1992).
[11] H. Z. Zhou and B. Bagchi, J. Chem. Phys. **97**, 3610 (1992).
[12] A. Papazyan and M. Maroncelli, J. Chem. Phys. **95**, 9219 (1991).
[13] A. Grossfield, J. Sachs, and T. B. Woolf, Proteins **41**, 211 (2000).
[14] R. F. Loring and S. Mukamel, J. Chem. Phys. **87**, 1272 (1987).
[15] B. Bagchi, A. Chandra, and S. A. Rice, J. Chem. Phys. **93**, 8991 (1990).
[16] B. Bagchi and A. Chandra, Phys. Rev. Lett. **64**, 455 (1990).
[17] C. Hu, V. N. Vovikov, and M. D. Fayer, J. Chem. Phys. **118**, 2800 (2003).
[18] S. Taraphder, J. Chem. Phys. **109**, 4948 (1998).
[19] R. Rosenberg and M. Lax, J. Chem. Phys. **21**, 424 (1953).
[20] M. Lax, J. Chem. Phys. **20**, 1351 (1952).
[21] R. A. Toupin and M. Lax, J. Chem. Phys. **27**, 458 (1957).
[22] U. M. Titulaer and J. M. Deutch, J. Chem. Phys. **60**, 2703 (1978).
[23] J. N. Onuchich and P. G. Wolynes, J. Chem. Phys. **98**, 2218 (1993).
[24] C. D. Eads, J. Phys. Chem. B **106**, 12282 (2002).
[25] I. Kusaka and D. W. Oxtoby, J. Chem. Phys. **115**, 4883 (2001).
[26] A. Erzan and G. Stell, Phys. Rev. B **18**, 408 (1978).
[27] J. S. Høye and G. Stell, Mol. Phys. **86**, 707 (1995).
[28] G. Nienhuis and J. M. Deutch, J. Chem. Phys. **56**, 5511 (1972).
[29] R. H. Cole, Mol. Phys. **27**, 1 (1974).
[30] B. J. Berne, J. Chem. Phys. **62**, 1154 (1975).
[31] D. J. Adams and I. R. McDonald, Mol. Phys. **32**, 931 (1976).
[32] S. Romano, Nuovo Cimento D **7**, 717 (1986).
[33] J. Wu and J. Cao, Phys. Rev. E **67**, 061116 (2003).
[34] J. Wu and J. Cao (unpublished).
[35] A. Papazyan and M. Maroncelli, J. Chem. Phys. **98**, 6431 (1993).
[36] J. M. Kosterlitz and D. J. Thouless, J. Phys. C **6**, 1181 (1973).
[37] J. V. Jóse and L. P. Kadanoff, Phys. Rev. B **16**, 1217 (1977).
[38] J. E. R. Costa and B. V. Costa, Phys. Rev. B **57**, 510 (1998).
[39] P. G. Debenedetti and F. H. Stillinger, Nature (London) **410**, 259 (2001).
[40] R. Zwanzig, Proc. Natl. Acad. Sci. U.S.A. **85**, 2020 (1988).
[41] L. M. Castro, A. S. T. Pires, and J. A. Plascak, J. Magn. Magn. Mater. **248**, 62 (2002).
[42] D. P. Landau, J. Appl. Phys. **73**, 6091 (1993).
[43] B. Zheng, M. Schulz, and S. Trimper, Phys. Rev. E **59**, R1351 (1999).
[44] J. T. Hynes and J. M. Deutch, in *Physical Chemistry (An Advanced Treatise)*, edited by D. Henderson (Academic, New York, 1975), Vol. XIB, pp. 729–836.